Development of Potent and Selective Inhibitors of *ecto*-5′-Nucleotidase Based on an Anthraquinone Scaffold

Younis Baqi,[†] Sang-Yong Lee,[†] Jamshed Iqbal,[†,||] Peter Ripphausen,[†,‡] Anne Lehr,[†] Anja B. Scheiff,[†] Herbert Zimmermann,[§] Jürgen Bajorath,[‡] and Christa E. Müller*,[†]

[†]*PharmaCenter Bonn, Pharmaceutical Institute, Pharmaceutical Chemistry I, Pharmaceutical Sciences Bonn (PSB), University of Bonn, An der Immenburg 4, D-53121 Bonn, Germany,* [‡]*Life Science Informatics, B-IT, LIMES−Chemical Biology and Medicinal Chemistry, University of Bonn, Dahlmannstrasse 2, 53113 Bonn, Germany, and* [§]*AK Neurochemie, Biozentrum der J.W. Goethe-Universität Frankfurt, Frankfurt am Main, Germany.* [||]*On leave from the Department of Pharmaceutical Sciences, COMSATS Institute of Information Technology Abbottabad, Pakistan.*

ecto-5′-Nucleotidase (*e*N, CD73) plays a major role in controlling extracellular adenosine levels. *e*N inhibitors have potential as novel drugs, for example, for the treatment of cancer. In the present study, we synthesized and investigated a series of 55 anthraquinone derivatives as potential inhibitors of *e*N, 11 of which are novel compounds and another 11 of which had previously been described but have now been synthesized by an improved method. We identified several potent inhibitors of rat *e*N. The most potent compounds were 1-amino-4-[4-fluoro-2-carboxyphenylamino]-9,10-dioxo-9,10-dihydroanthracene-2-sulfonate (**45**, PSB-0952, $K_i = 260$ nM) and 1-amino-4-[2-anthracenylamino]-9,10-dioxo-9,10-dihydroanthracene-2-sulfonate (**52**, PSB-0963, 150 nM), with **52** being the most potent *e*N inhibitor described to date. Selected compounds were further characterized and found to exhibit a competitive mechanism of inhibition. Investigations of *ecto*-nucleoside triphosphate diphosphohydrolases (NTPDases) and the P2Y receptor subtypes P2Y$_2$, P2Y$_4$, P2Y$_6$, and P2Y$_{12}$ showed that compound **45** exhibited the highest degree of selectivity (>150-fold).

Introduction

The purine nucleoside adenosine and its nucleotides ATP and ADP and the pyrimidine nucleotides UTP and UDP play a critical role in the central and peripheral nervous system. They act as extracellular messengers regulating cell functions by activating P1 (adenosine) or P2 (nucleotide) receptors.[1] Furthermore, the nucleobase adenine has recently been identified as a signaling molecule activating specific G protein-coupled adenine receptors (P0 receptor).[2] ATP can be released as a cotransmitter together with acetylcholine, norepinephrine, glutamate, γ-aminobutyric acid, or peptide neurotransmitters.[3] Once released, in addition to interacting directly with P2 receptors (P2Y or P2X subtypes), ATP can be hydrolyzed by a family of ectonucleotidases.[4] Nucleotide triphosphate diphosphohydrolases (NTPDases) catalyze the sequential hydrolysis of the β- and γ-phosphate of adenosine and uridine nucleoside di- and triphosphates,[5] the physiological ligands of P2 receptors. Three distinct nucleotide pyrophosphatase subtypes (NPP1,2,3) hydrolyze ATP directly to AMP and pyrophosphate (PP$_i$). *ecto*-5′-Nucleotidase [*e*N, cluster of differentiation 73 (CD73)][a] finally converts AMP to adenosine and other nucleoside monophosphates to the corresponding nucleosides. *e*N is anchored in the plasma membrane by means of a glycosylphosphatidylinositol anchor.[6] It can also be cleaved off and keeps its enzymatic activity in the soluble form.[6] The main function of *e*N is the hydrolysis of AMP to adenosine. It is thus part of the cascade (together with NTPDases) to terminate the action of nucleotides such as ATP as extracellular signaling molecules acting on P2 (P2X and P2Y) receptors.[7] On the other hand, the enzyme generates adenosine, which acts on P1 receptors. There is evidence for a coordinated induction and repression of *e*N and the A$_{2A}$ adenosine receptor in human B-cell lines.[8] The enzyme is also important for the recycling of extracellular nucleotides, which are converted to nucleosides by *e*N and internalized through specific nucleoside transporters.[6,9] *e*Ns have been reported to be highly expressed in melanoma cells, and the *e*N levels have been associated with their ability to metastasize.[10] *e*N and adenosine are involved in immune responses, for example, involving T-cell and B-cell,[11] and in tumor promotion[12] and multidrug resistance.[13] Potential applications of *e*N inhibitors include therapies that aim at reducing adenosine concentrations in a site- and event-specific manner at sites where it is formed by breakdown of extracellular nucleotides. Thus, *e*N inhibitors have been proposed as novel therapeutics for cancer including melanomas,[10] gliomas,[14] and breast cancers.[15] In addition, *e*N inhibitors may be useful in the treatment of gastrointestinal infections

---

*To whom correspondence should be addressed. Tel: +49-228-73-2301. Fax: +49-228-73-2567. E-mail: christa.mueller@uni-bonn.de.

[a]Abbreviations: AB-25, Acid Blue 25; AOPCP, β-methylene-ADP (adenosine-5′-phosphorylmethylphosphonic acid); AMBER, Assisted Model Building with Energy Refinement; CD73, cluster of differentiation 73; CE, capillary electrophoresis; *e*N, *ecto*-5′-nucleotidase (= CD73); (E)-NTPDase, (*ecto*)-nucleoside 5′-triphosphate diphosphohydrolase; ESI, electrospray ionization; HPLC, high-performance liquid chromatography; LC-MS, liquid chromatography−mass spectrometry; MOE, Molecular Operating Environment; NMR, nuclear magnetic resonance; NPP, nucleotide pyrophosphatase; PDB, Protein Data Bank; RB-2, Reactive Blue 2; SARs, structure−activity relationships; TLC, thin-layer chromatography; vdW, van der Waals.

Published on Web 02/10/2010
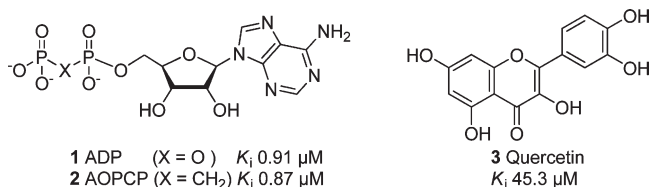
Figure 1. Structure of the *e*N inhibitors: ADP (**1**), AOPCP (**2**), and quercetin (**3**).
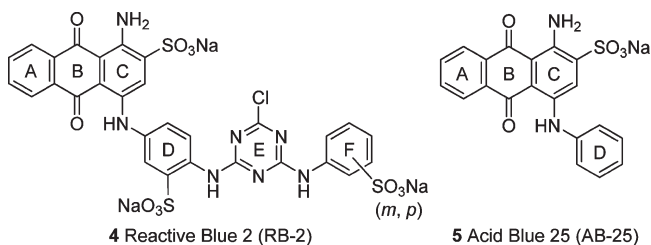

Figure 2. Structure of RB-2 and AB-25.

and bacterial diarrhea[16] and the treatment of hepatic fibrosis.[17]

Only a few inhibitors of *e*N have been described to date. ADP (**1**) is a moderately potent inhibitor ($K_i = 0.91$ μM).[18] The currently used standard inhibitor is an analogue of **1**, in which the β-phosphate ester bond is replaced by a methylene group (β-methylene-ADP, AOPCP, **2**, Figure 1). The compound is a nucleotide analogue bearing negative charges at physiological pH value and can therefore not be perorally absorbed. In addition, it may be hydrolyzed to yield the adenosine receptor agonist adenosine. Besides **2**, some natural products—polyphenols[19] including the flavonoid quercetin (**3**)[20]—have been described as weak inhibitors of *e*N (for K_i values, see Figure 1).

The anthraquinone dye Reactive Blue 2 (RB-2, **4**, Figure 2) has been reported to act as a nonselective antagonist of nucleotide receptors (P2X$_1$, P2X$_2$, P2X$_4$, P2Y$_1$, P2Y$_2$, P2Y$_4$, P2Y$_6$, P2Y$_{11}$, and P2Y$_{12}$ receptors)[21−34] and as a nonselective inhibitor of NTPDases.[35] Thus, compound **4** seems to exhibit high affinity for protein sites normally associated with the binding of nucleotides. In our search for potent *e*N inhibitors, we discovered that **4** was a relatively potent, although non-selective, inhibitor of the enzyme showing a K_i value of 3.07 μM (Table 2 and Figure 2). Furthermore, we found that the much smaller anilinoanthraquinone derivative **5** (1-amino-4-phenylamino-9,10-dioxo-9,10-dihydroanthracene-2-sulfo-nate) also known as Acid Blue 25 (AB-25) was only 5-fold less potent ($K_i = 15.2$ μM, Figure 2 and Table 2), indicating that a relatively small substituent in the 4-position of the anthraqui-none ring system would be sufficient. Like compound **4**, **5** has been shown to interact with a number of nucleotide-binding targets and thus is not selective for *e*N.[22b,32,35] However, because of its small size, it could be a suitable starting point for studying structure−activity relationships (SARs) and to optimize this scaffold with respect to *e*N affinity and selecti-vity. It had previously been shown that the substitution pattern in the 4-position of the anthraquinone moiety plays an important and critical role for the ability of the compounds to antagonize P2Y receptor subtypes, such as P2X$_1$ and P2Y$_1$-like,[36] P2Y$_2$,[32] and P2Y$_{12}$ receptors,[33,34] and to inhibit NTPDase isoenzymes.[35] The modification of this substituent has, for example, led to the development of the most potent

Scheme 1. General Synthesis of 4-Substituted Anthraquinone Derivatives[a,b]
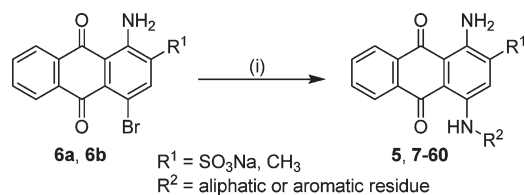
[a] Reagents and conditions: (i) R^2−NH$_2$, phosphate buffer, pH 6−7, Cu^0, microwave, 100−120 °C, 5−24 min. [b] For R^1 and R^2, see Table 2.

non-nucleotide-derived P2Y$_{12}$ antagonists known to date, which exhibit high selectivity versus other P2 receptors as well as versus *ecto*-nucleotidases.[33,34]

Thus, the anthraquinone scaffold appears to behave as a privileged structure in medicinal chemistry[37] for nucleotide-binding protein targets—similarly to the xanthine scaffold (lead structure: caffeine) that had been extremely useful for developing selective adenosine receptor antagonists for all four receptor subtypes, as well as selective inhibitors for a number of other protein targets.[38]

In the present study, we identified a new class of *e*N inhibitors derived from the anilinoanthraquinone derivative **5** and related to RB-2 (**4**). The compounds were optimized by structural modification, and SARs were analyzed with the goal to obtain potent and selective *e*N inhibitors.

Results and Discussion

Chemistry. The anthraquinone derivatives were synthe-sized as depicted in Scheme 1. The syntheses of compounds **5**, **7−10**, **15−20**, **22−25**, **27−29**, **31−43**, **46**, and **49** have pre-viously been described.[32,34,35] Compounds **12−14**, **21**, **26**, **30**, **47**, **50**, and **53−55**, whose syntheses had previously been described by classical methods,[35,39−48] as well as the new compounds **11**, **44**, **45**, **48**, **51**, **52**, and **56−60** were obtained in analogy to a new method recently developed by our group applying a simple and efficient microwave-assisted Ullmann reaction (Scheme 1).[49] Our experiments showed that a wide variety of amines (aliphatic and aromatic) including highly electron-deficient ones could be smoothly coupled with anthraquinone halide derivatives **6**. Treatment of 4-bromo-substituted anthraquinone derivatives (**6a**, bromaminic acid: R^1 = SO$_3$H; **6b**, 1-amino-4-bromo-2-methylanthraquinone: R^1 = CH$_3$) with diversely substituted amines in phosphate buffer (pH 6−7) in the presence of a catalytic amount of copper powder (Cu^0) under microwave irradiation at 100−120 °C for 5−24 min yielded the target compounds in moderate to excellent yields (Scheme 1 and Table 1).

The compounds were purified by flash column chroma-tography on reversed phase material. The purity of the compounds was determined by high-performance liquid chromatography (HPLC)-MS/UV methods, and a purity of at least 95% was confirmed.

Enzyme Inhibiton Assays. The enzymatic reaction was performed essentially as described previously.[50,51] A rela-tively high substrate concentration of 500 μM was used due to the low sensitivity of the capillary electrophoresis (CE)-UV method used to quantify the reaction product adenosine. Inhibitors did not comigrate with adenosine and thus did not interfere with the detection of the product of the enzymatic reaction. The test compounds were initially screened at a

Table 1. Reaction Time, Isolated Yield, Molecular Weight (MW), and Purity by LC-MS of the Newly Synthesized Anthraquinone Derivatives
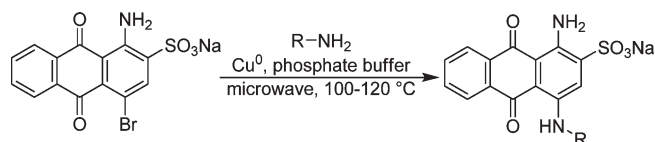
compd	R	reaction time (min)	yield (%)[a]	MW (g/mol)	purity by LC-MS/UV (%)[b]
11	4-chlorophenethyl	15	28	478.9	99.4
12	isopropyl	5	90	382.4	99.2
13	cyclopentyl	24	32	408.4	98.1
14	cyclohexyl	24	38	421.5	99.7
21	3-amino-2,4,6-trimethylphenyl	5	40	473.5	95.0
26	4-phenoxyphenyl	10	30	508.5	97.7
30	4-bromophenyl	20	60	495.3	99.2
44	4-(diethoxyphosphoryl)methylphenyl	5	68	566.5	98.4
45	2-carboxy-4-fluorophenyl	5	70	478.5	97.0
47	4-bromo-2-carboxyphenyl	5	75	539.5	98.9
48	2-carboxy-5-fluorophenyl	5	60	478.5	98.5
51	6-carboxy-2-naphthyl	5	45	510.5	99.2
52	2-anthracenyl	5	10	516.5	96.5
54	5-sulfo-1-naphthyl	5	30	568.5	98.0
55	6-sulfo-1-naphthyl	5	35	568.5	99.6
56	7-sulfo-1-naphthyl	5	25	568.5	95.8
57	8-sulfo-1-naphthyl	5	28	568.5	96.0
58	2-methyl-1-naphthyl	20	50	480.5	99.4
59	1-anthracenyl	5	10	516.5	96.5
60	9-phenanthrenyl	5	15	516.5	96.6

[a] Isolated yield. [b] A sample (10 μL) was injected into an HPLC column and elution was performed with a gradient of water: methanol (containing 2 mM NH_4CH_3COO) from 90: 10 to 0: 100 for 30 min at a flow rate of 250 μL/min, starting the gradient after 10 min. UV absorption was detected from 200 to 950 nm using a diode array detector. Purity of the compounds was determined at 254 nm.
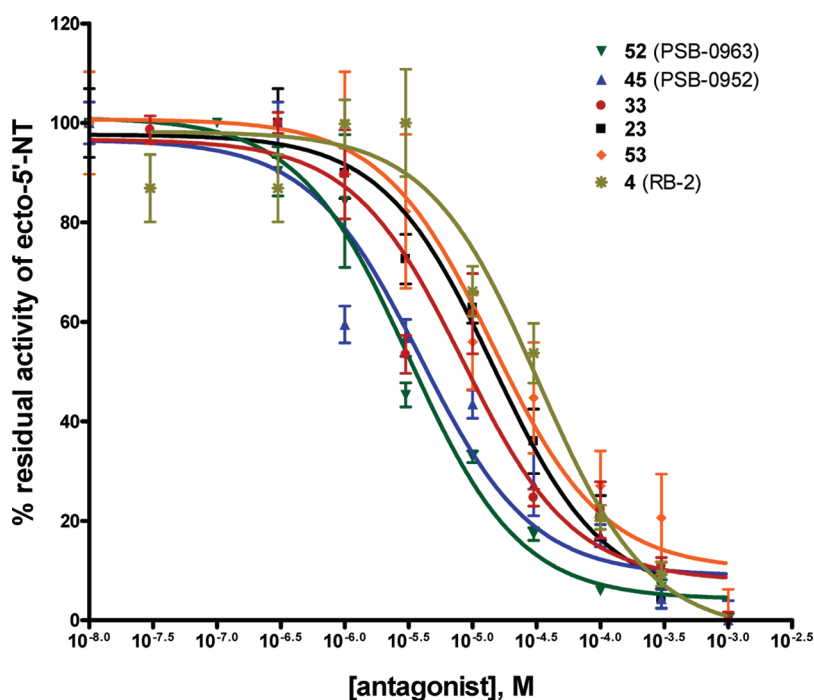
Figure 3. Concentration−response curves for selected, potent eN inhibitors **23**, **33**, **45**, **52**, and **53** and the parent compound RB-2 (**4**). Rat enzyme K_m, 20 μM; AMP concentration, 500 μM. Data points are from three separate experiments performed in duplicate.

high concentration of 1 mM. For compounds that showed high inhibition at that concentration (typically > 50−60%), full concentration−inhibition curves were determined, and K_i values were calculated from the obtained IC_{50} values. Concentration−inhibition curves for selected compounds are depicted in Figure 3.

SARs. RB-2 (**4**) is a well-known compound that binds to almost all P2 receptor subtypes as well as to various *ecto*-nucleotidases. It inhibited eN with a K_i value of 3.07 μM. Anthraquinone derivative **5**, a much smaller molecule as compared to RB-2, showed a moderate inhibitory potency at eN with a K_i value of 15.2 μM. Both **4** and **5** are not selective

for any purinergic target on which they have been tested so far. Nevertheless, **5** is a better starting compound than **4** for several reasons: (i) It has a low molecular weight; (ii) a large number of analogues can easily be synthesized allowing the analysis of SARs of this very promising anthraquinone-containing scaffold; and (iii) it has only one sulfonate group, which might easily be replaced by a bioisosteric group, such as tetrazole or carboxylate, while **4** has three sulfonate functions.

A sulfonate group in position 2 of the anthraquinone moiety of compound **5** appeared to be essential for *e*N inhibitory activity; when this group was replaced by a methyl group as in compound **7**, the inhibitory activity was lost (Table 2). Compound **5** contains an unsubstituted phenylamino ring in the C-4 position. Replacement of the phenylamino ring by benzylamino, phenethylamino, 4′-chlorophenethylamino, or 3′,4′-dimethoxyphenethylamino (**8**−**11**) dramatically decreased the inhibitory activity (Table 2). Likewise, the replacement of the aromatic residues by aliphatic groups like isopropyl or cyclopentyl (**12** and **13**) reduced or nearly abolished the activity. Interestingly, the cyclohexylamino-substituted anthraquinone derivative **14** showed a relatively high inhibitory activity ($K_i = 1.66 \, \mu$M).

The introduction of a lipophilic methyl group in the *o*- or *p*-position (**15** and **17**) led to a reduced activity (Table 2). For example, the *p*-methyl derivative **17** showed a high K_i value of 360 μM. It can be concluded that a hydrophobic substituent in the *o*- or *p*-position of the phenyl ring of **5** decreased the inhibitory activity, while it was somewhat better tolerated in the *m*-position (compound **16**). As expected, neither dimethyl substitution showed any improvement in the activity (**18**−**20**) nor did a combination of three methyl groups (*o*, *o*, and *p*) with an amino group in the *m*-position (**21**).

The introduction of a hydroxyl group in the *o*- or *p*-position of the phenyl ring increasing the hydrophilicity led to a large increase in the potency of the compounds (**22** and **23**). The hydroxy group could form a hydrogen bond to the active site of the enzyme, possibly contributing to the high affinity. The potency was greatly reduced if the hydroxy group was methylated as in **24** or ethylated as in **25** and **27**. However, the activity was only moderately reduced when the *p*-hydroxy group was converted to an aromatic ether (phenoxyphenylamino, **26**). The possibility of $\pi-\pi$ interactions by **26** may partly compensate for the loss of the hydrogen donor function in **26**. The introduction of a halogen (fluorine, chlorine, or bromine) substituent in the *p*-position (**28**−**30**) led to potent inhibitors, which, however, did not reach the potency of the *o*- or *p*-hydroxy derivatives **22** and **23**. The introduction of an amino group in the *p*-position of the phenyl ring (compound **33**) increased the hydrophilicity and had a strong impact on the inhibitory activity. In fact, the *p*-amino-substituted compound **33** was similarly potent as the *p*-hydroxy derivative **23**, both of which have a hydrogen bond donor function. In contrast, introducing an amino group in the *o*- or *m*-position (**31** and **32**) reduced the inhibitory activity. The activity was dramatically reduced when the amino function in the *p*-position was substituted by a phenyl residue (phenylamino-substituted derivative **37**). This was probably due to the loss of the hydrogen bond donor function (*p*-amino). The introduction of a sulfonate group in the *m*-position in addition to a *p*-amino group (**35**) led to a decrease in the activity of more than 30-fold as compared with **33**. Exchange of the position

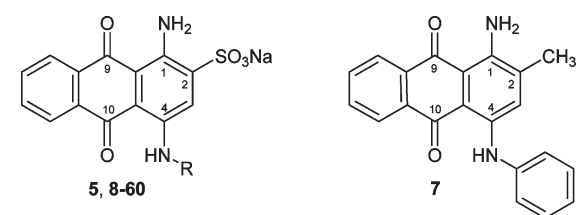of the amino and sulfonate residue (**34**) reduced the activity.

The introduction of a carboxylate function in the *o*-, *m*-, or *p*-position of the phenyl ring (**38**−**40**) was subsequently investigated. A carboxylate group in the *m*- or *p*-position (**39** and **40**) decreased the activity, while a carboxylate in the *o*-position (**38**) caused an increase in the inhibitory activity. The exchange of the carboxylate function by a sulfonate group in the *o*-position (**41**) led to a further reduction in activity, while exchange of carboxylate by sulfonate in the *p*-position (**42**) increased the activity. Furthermore, we observed that larger polar substituents in the *p*-position as in compounds **43** and **44** decreased the activity.

The combination of an *o*-carboxylate as in **38** with a *p*-halogen group (see **28**−**30**) was tested since the respective monosubstituted derivatives were relatively potent. However, only in the case of a *p*-fluorine substitution (**45**), a potent disubstituted compound was obtained (**45**, $K_i = 0.26$ μM). If the fluorine atom was replaced by the much larger halogen atoms chlorine or bromine (**46** and **47**), the activity was dramatically decreased. A combination of *o*-carboxy with *m*-fluoro or *m*-chloro substitution (**48** and **49**) also led to only weakly active compounds; again, the smaller fluorine atom was somewhat better tolerated than chloro substitution.

The replacement of the phenyl ring (in **5**) by β-naphthalene (**50**, $K_i = 1.47$ μM) or α-naphthalene (**53**, $K_i = 0.53$ μM) increased the inhibitory activity. Enlargement of the aromatic ring system increases $\pi-\pi$ interactions and thus the potency of the anthraquinone derivatives. The enzyme appears to contain a hydrophobic pocket that can interact with the aromatic rings. Additional hydrophilic substituents, for example, carboxylation of the β-naphthyl at the 5-position (**51**), sulfonation of the α-naphthyl ring in positions 5, 6, 7, or 8 (**54**−**57**), or methylation of the α-naphthyl in position 2 (**58**), did not improve the inhibitory activity; in contrast, it even reduced activity, in some cases to a large extent. In particular, sulfonation in position 7 of the α-naphthyl ring (**56**) led to complete inactivity of the resulting molecule. Interestingly, the (formal) combination of α- and β-naphthyl substitution in the phenanthrenyl-substituted compound **60** abolished activity. The exchange of α-naphthyl (**53**) by α-anthracenyl (**59**) led to a slight reduction in activity (from 0.53 to 2.93 μM), while the replacement of β-naphthyl (**50**, $K_i = 1.47$ μM) by β-anthracenyl (**52**, $K_i = 0.15$ μM) led to a 10-fold increase in affinity. Compound **52** is the most potent inhibitor of *e*N known to date. Thus, the β-anthracenyl residue seems to fit ideally into the hydrophobic pocket of *e*N and may interact with aromatic amino acid residues.

Figure 4 summarizes typical features required for *e*N inhibition. Besides an acidic functional group in the 2-position of the anthraquinone core, the enzyme features a large hydrophobic pocket in the region of the 4-position. Large aromatic annelated rings, such as naphthalene or anthracene, can be accommodated. In the case of a phenyl ring, hydrogen bond-donating groups (OH and NH_2) in the *p*-position and polar groups (CO_2H and OH) in the *o*-position were favorable.

It is possible that different binding modes exist for compounds exhibiting a hydrophobic 4-substituent on the one hand and compounds with polar groups at the same position on the other hand. To gain more insight into the binding of anthraquinone derivatives to *e*N, we subsequently investigated their mechanism of enzyme inhbition and docked the

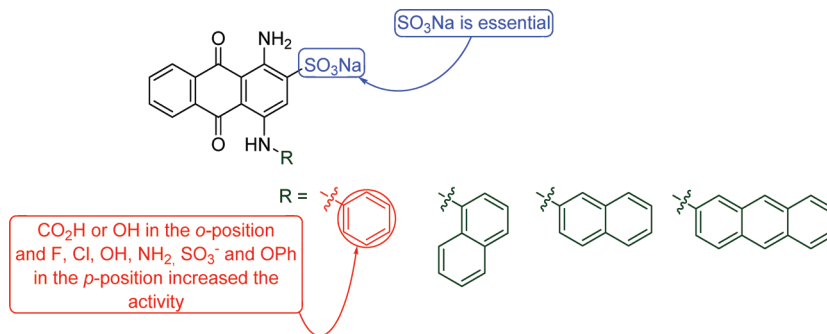**Table 2.** Potency of Anthraquinone Derivatives as *e*N Inhibitors

compd	R	$K_i \pm$ SEM (μM) (or % inhibition at 1 mM concentration)[a]
4 (RB-2)	see Figure 2	**3.07 $\pm$ 0.24**
5 (AB-25)	phenyl	**15.2 $\pm$ 0.95**
7	for structure, see above	(4 $\pm$ 4%)
8	benzyl	(43 $\pm$ 2%)
9	phenethyl	(53 $\pm$ 7%)
10	3,4-dimethoxyphenethyl	(44 $\pm$ 1%)
11	4-chlorophenethyl	(62 $\pm$ 9%)
12	isopropyl	(15 $\pm$ 5%)
13	cyclopentyl	(51 $\pm$ 12%)
14	cyclohexyl	**1.66 $\pm$ 0.24**
15	2-methylphenyl	(33 $\pm$ 1%)
16	3-methylphenyl	**12.3 $\pm$ 3.7**
17	4-methylphenyl	**360 $\pm$ 22**
18	2,3-dimethylphenyl	(39 $\pm$ 2%)
19	2,4-dimethylphenyl	(47 $\pm$ 2%)
20	2,5-dimethylphenyl	(26 $\pm$ 5%)
21	3-amino-2,4,6-trimethylphenyl	**36.0 $\pm$ 1.4**
22	2-hydroxyphenyl	**1.84 $\pm$ 0.02**
23	4-hydroxyphenyl	**0.62 $\pm$ 0.15**
24	2-methoxyphenyl	(9 $\pm$ 1%)
25	4-ethoxyphenyl	(31 $\pm$ 9%)
26	4-phenoxyphenyl	**1.51 $\pm$ 0.40**
27	2-ethoxyphenyl	(56 $\pm$ 4%)
28	4-chlorophenyl	**4.81 $\pm$ 0.34**
29	4-fluorophenyl	**5.67 $\pm$ 1.90**
30	4-bromophenyl	**11.3 $\pm$ 2.2**
31	2-aminophenyl	(47 $\pm$ 12)
32	3-aminophenyl	(31 $\pm$ 11%)
33	4-aminophenyl	**0.297 $\pm$ 0.092**
34	3-amino-4-sulfophenyl	**25.2 $\pm$ 10.3**
35	4-amino-3-sulfophenyl	**10.0 $\pm$ 3.82**
36	3-amino-5-carboxyphenyl	(44 $\pm$ 5%)
37	4-phenylaminophenyl	(37 $\pm$ 10%)
38	2-carboxyphenyl	**6.53 $\pm$ 0.48**
39	3-carboxyphenyl	(26 $\pm$ 4%)
40	4-carboxyphenyl	(34 $\pm$ 6%)
41	2-sulfophenyl	(14 $\pm$ 6%)
42	4-sulfophenyl	**3.43 $\pm$ 0.62**
43	4-carboxymethylphenyl	(26 $\pm$ 4%)
44	4-(diethoxyphosphoryl)methylphenyl	(28 $\pm$ 3%)
45	2-carboxy-4-fluorophenyl	**0.26 $\pm$ 0.01**
46	2-carboxy-4-chlorophenyl	(52 $\pm$ 4%)
47	4-bromo-2-carboxyphenyl	(56 $\pm$ 1%)
48	2-carboxy-5-fluorophenyl	(60 $\pm$ 20%)
49	2-carboxy-5-chlorophenyl	(27 $\pm$ 1%)
50	2-naphthyl	**1.47 $\pm$ 0.33**
51	6-carboxy-2-naphthyl	**3.43 $\pm$ 0.62**
52	2-anthracenyl	**0.15 $\pm$ 0.02**
53	1-naphthyl	**0.53 $\pm$ 0.03**
54	5-sulfo-1-naphthyl	**11.7 $\pm$ 0.6**
55	6-sulfo-1-naphthyl	**15.3 $\pm$ 0.8**
56	7-sulfo-1-naphthyl	(0 $\pm$ 0%)
57	8-sulfo-1-naphthyl	**6.05 $\pm$ 1.51**
58	2-methyl-1-naphthyl	**2.74 $\pm$ 0.75**
59	1-anthracenyl	**2.93 $\pm$ 0.12**
60	9-phenanthrenyl	(58 $\pm$ 5%)

[a] Three separate experiments were performed, each in duplicate.

compounds into the binding site of a homology model of the enzyme (see below).

Mechanism of Inhibition. Two of the most potent compounds, the anthracenyl derivative **52** and the α-naphthyl derivative **53**, were further investigated to determine their mechanism of inhibition. Thus, enzyme kinetics were determined in the absence and in the presence of various concentrations of inhibitor. It was found that the V_{max} value did not significantly change in the presence of the inhibitors, while the K_m value increased with increasing inhibitor concentrations, indicating that **52** and **53** exhibit a competitive mechanism of inhibition. Figure 5 shows the Michaelis–Menten and the Lineweaver–Burk plots for compound **53**. The Lineweaver–Burk plot visualizes the competitive mechanism of inhibition by showing the same *y*-intercept for uninhibited and inhibited enzyme. However, the data obtained by the applied CE method are not accurate enough to completely exclude a mixed type of inhibition.

Molecular Modeling Studies. We have investigated how the strongest inhibitor, compound **52**, might bind to the active site of *e*N using a comparative molecular model of rat *e*N. This model was built based on the crystal structure of 5′-nucleotidase precursor (5′-NP) from *Thermus thermophilus* HB8[52] [Protein Data Bank (PDB) code: 2Z1A, 34.8% sequence identity] as a modeling template using standard comparative modeling techniques available in the Molecular Operating Environment (MOE 2007.9).[53] In the active site region, the model is thought to be a reasonable approximation of the *e*N structure because the residues forming the active sites in the template and *e*N are mostly identical, with only four exceptions [Phe481 (5′-NP)/Tyr502 (*e*N), Arg345/Ala352, Trp277/Phe285, and His240/Asn247]. The only nonconservative mutation in the active site region is the Arg345/Ala352 change. However, Arg345 maps to a partly solvent-exposed position in the crystal structure of the template; hence, significant conformational effects as a consequence of this mutation are unlikely. The model was built in the presence of the *e*N standard inhibitor AOPCP (**2**, Figure 1). This inhibitor could be built into the model because the template had been cocrystallized with a structural analogue of **2**, from which the inhibitor position could be inferred. Because compound **52** is a larger molecule than **2** to which the active site in the model was adapted, we superimposed compound **52** onto the structurally corresponding parts of **2**. Specifically, the anthracene moiety was aligned with the purine and ribose groups of **2** and the sulfonate group of the inhibitor with the terminal phosphate group of **2** in its crystallographic position. This pose represented the only plausible orientation of the inhibitor within the binding site. Residues in the model within 4.5 Å of compound **52** were then subjected to limited energy minimization using MOE, except the two zinc coordination spheres that were held fixed (see the Experimental Section). Only minor changes in atomic positions of a few active site residues were required to adapt to the larger inhibitor in its crystallographically oriented pose, quasi as a modeled "induced fit", and accommodate it without steric constraints. Flexible ligand docking of compound **52** into this adjusted active site using FlexX 2.2.1 with standard parameter settings (except a slight increase in overlap volume) essentially reproduced the manually modeled pose.[54,55] In its modeled position, the anthracene moiety of compound **52** stacks between Phe419 and Tyr502, the anthraquinone group fits into a hydrophobic pocket, and the essential sulfonate group is positioned to

Figure 4. SARs of anthraquinone derivatives as *e*N inhibitors.
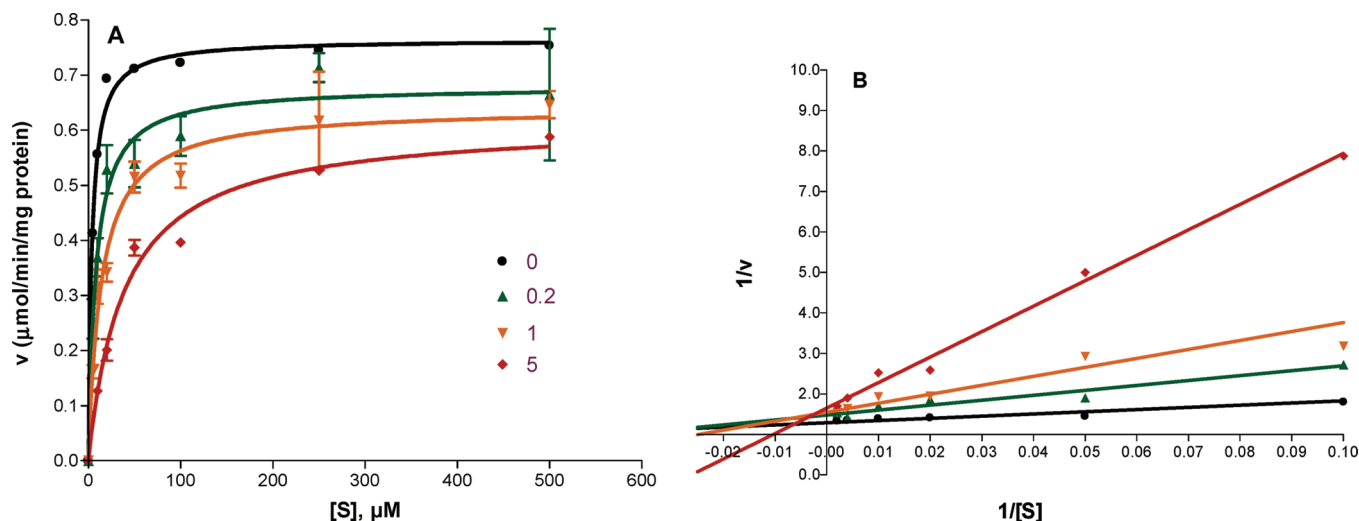
Figure 5. (A) Michaelis−Menten plot and (B) Lineweaver−Burk plot of rat *e*N inhibition by compound **53**. S, concentration of substrate AMP (μM); concentration of **53**: black circle, 0 μM; green triangle, 0.2 μM; yellow triangle, 1 μM; and red diamond, 5 μM.

interact with one of the divalent zinc ions of the enzyme (see Figure 6). Thus, despite the general uncertainties associated with binding mode predictions, the modeled binding mode of compound **52** is plausible and qualitatively consistent with strong inhibition.

Selectivity. Selected compounds were further investigated at several purinergic targets including other *ecto*-nucleotidases (*ecto*-NTPDases 1, 2, and 3) and P2Y receptor subtypes PY$_2$, P2Y$_4$, P2Y$_6$, and P2Y$_{12}$ (see Tables 3 and 4). The lead compound **4** is nonselective: It is 7−8-fold less potent at NTPDase1 and 2 but 3-fold more potent at NTPDase 3 as compared to *e*N (Table 3). Compound **4** also interacts with various P2Y receptor subtpyes at low micromolar or submicromolar concentrations (Table 4). The smaller anilinoanthraquinone derivative **5** was similarly nonselective.

The α-naphthylaminoanthraquinone derivative **53**, which had previously been shown to be a relatively selective inhibitor of NTPDase3 in rat with a K_i value of 1.5 μM,[35] was now found to be even 3-fold more potent as an inhibitor of *e*N (K_i = 0.53 μM). It appears that the binding site of NTPDase3 like that of *e*N features a hydrophobic pocket that accommodates flat aromatic ring systems. However, the β-anthracenyl-substituted compound **52**, which was the most potent *e*N inhibitor, was also relatively selective: The larger aromatic substituent was no longer tolerated by NTPDase3; it was also inactive at NTPDase2 and showed some affinity for NTPDase1 but was still 17-fold selective for *e*N vs NTPDase1 (Table 3). The compound did not show affinity for the investigated P2Y receptor subtypes (Table 4).

Anthraquinone derivative **45**, the second most potent compound of the present series, was > 150-fold selective versus NTPDases as well as P2Y receptors.

It had recently been shown that anthraquinone derivatives are suitable scaffolds for developing very potent and selective antagonists for the platelet P2Y$_{12}$ receptor subtype;[33,34] the present results now show that anthraquinones can also be optimized toward affinity and selectivity for other nucleotide-binding proteins, namely, the AMP-hydrolyzing *ecto*-enzyme *e*N.

Toxicity. Several hydroxyl-substituted anthraquinone derivatives bearing basic side chains are known to intercalate into DNA, tightly bind to the negatively charged nucleic acid, inhibit the DNA-topoisomerase II complex, and may finally lead to the damage of DNA by the formation of reactive oxygen species.[56] Such compounds, for example, doxorubicin and mitoxanthrone, are therefore used as potent anticancer drugs.[56] They also exhibit mutagenic, carcinogenic, and cardiotoxic properties.[56] However, the toxic effects are strongly dependent on the substitution pattern, and many anthraquinone derivatives, namely, those lacking phenolic functions and/or basic side chains, have been found to be nontoxic or may even exhibit antioxidant, antimutagenic, or other beneficial properties.[33,57−60] One of the most potent compounds of the present series, the anthracenylamino-substituted derivative **52**, belongs to the group of polyaromatic hydrocarbons (PAHs) for some of which carcinogenic properties have been described.[61] Anthracene itself has been tested for carcinogenicity in mice in several
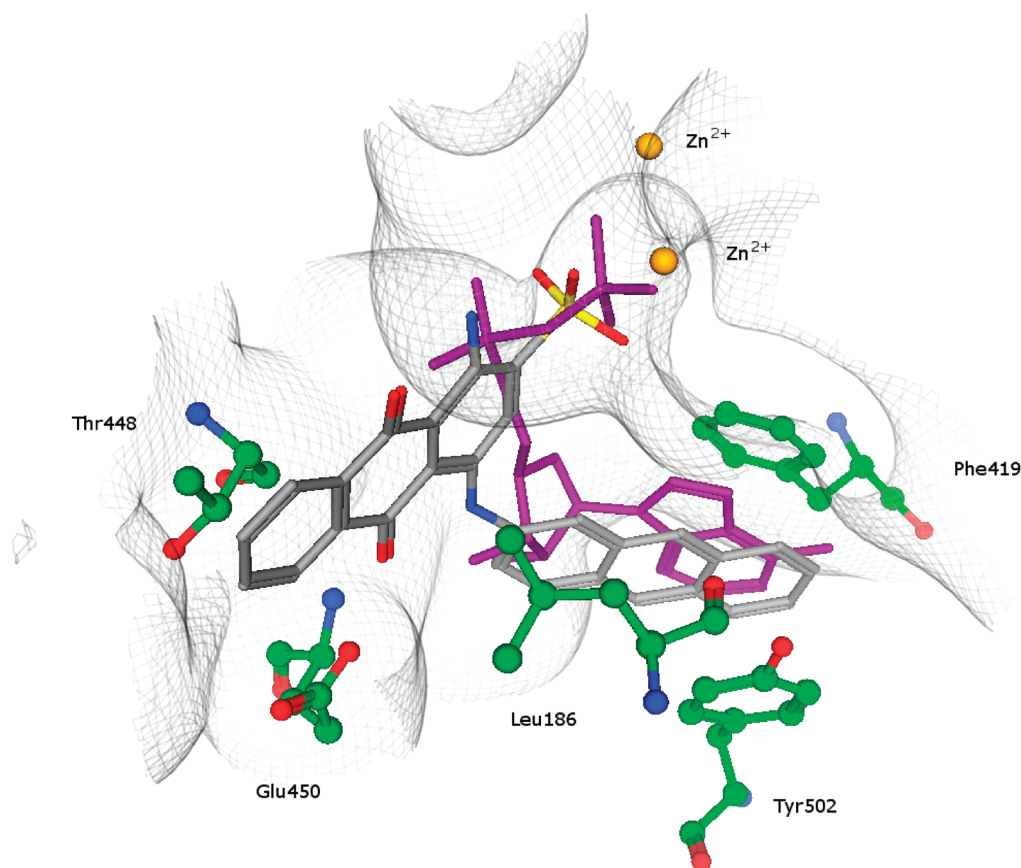
Figure 6. Model of compound **52** in the active site of rat *e*N. Shown is a superposition of compounds **52** and **2** within the active site of rat *e*N. Carbon atoms of the inhibitor **52** and *e*N residues are colored gray and green, respectively, oxygen atoms are red, and nitrogen atoms blue. ADP analogue **2** (AOPCP) is colored purple, and the two catalytic zinc ions are depicted as gold spheres.

Table 3. Inhibitory Potency of Selected *e*N Inhibitors at Nucleoside Triphosphate Diphosphohydrolases

	ecto-enzymes			
	$K_i \pm$ SEM (μM)			
compd	*e*N	NTPDase1	NTPDase2	NTPDase3
4, RB2	3.07 ± 0.24^{a}	20.0 ± 0.0^{a35}	24.2 ± 0.06^{a35}	1.10 ± 0.03^{a35}
5, AB-25	15.2 ± 0.95^{a}	49.1 ± 5.1^{a35}	35.8 ± 6.1^{a35}	14.3 ± 1.5^{a35}
23	0.62 ± 0.15^{a}	10.7 ± 0.5^{b}	$> 200^{b}$	ND^{c}
45	0.26 ± 0.01^{a}	$> 40^{b}$	$\gg 200^{b}$	$> 60^{b}$
52	0.15 ± 0.02^{a}	2.59 ± 1.37^{b}	$\gg 200^{b}$	$> 60^{b}$
53	0.53 ± 0.03^{a}	$\gg 150^{a35}$	$\gg 400^{a35}$	1.5 ± 0.1^{a35}

[a] Inhibiton measured at rat enzyme. *[b]* Inhibiton measured at human enzyme. *[c]* ND, not determined.

Table 4. Antagonistic Potency of Selected *e*N Inhibitors at Some P2Y Receptor Subtypes

		IC_{50} (μM)			$K_i \pm$ SEM (μM) vs [^{3}H]PSB-0413
compd	*e*N$^{a}K_i \pm$ SEM (μM)	P2Y$_2$^{b}	P2Y$_4$^{b}	P2Y$_6$^{a}	P2Y$_{12}$^{b}
4, RB-2	3.07 ± 0.24	1.85 ± 0.39	9.79 ± 3.91	4.34 ± 0.89	0.68 ± 0.26^{33}
5, AB-25	15.2 ± 0.95	11.0 ± 1.0	25.8 ± 14.3	$\gg 10$	9.83 ± 2.43^{33}
23	0.62 ± 0.15	4.63 ± 0.53	2.37 ± 1.12	5.30 ± 1.00	$\approx 10^{33}$
45	0.26 ± 0.01	29.9 ± 4.9	$\gg 10$	≈ 10	$> 10^{33}$
52	0.15 ± 0.02	≈ 10	> 10	$\gg 10$	ND^{c}
53	0.53 ± 0.03	6.67 ± 0.32	10.1 ± 1.4	~ 30	$> 10^{33}$

[a] Inhibition measured at enzyme or receptor from rat. *[b]* Human receptors. *[c]* ND, not determined.

studies and for mutagenicity in bacteria, yeast, and cultured mammalian cells.[61] However, no indication of carcinogenicity or mutagenicity was found.[61]

We have recently tested two of the anthraquinone derivatives identified in the present study as *e*N inhibitors, **28** and **53**, for their effects on human cancer cell lines: 1321N1

astrocytoma cells and 1539 melanoma cells.[33] In contrast to the anticancer drug 5-fluorouracil, which efficiently inhibited the proliferation of both cell lines, **28** and **53** did not show any effect in the MTT [3-(4,5-dimethylthiazol-2-yl)-2,5-diphenyltetrazolium bromide] test at concentrations up to 100 μM.[33] These results indicated that they were not

cytotoxic and did not inhibit mitochondrial activity of the cells.[33]

In the present study, both investigated compounds have been found to be relatively potent *e*N inhibitors (K_i: **28**, 4.81 μM; **53**, 0.53 μM). It had previously been shown that 1539 melanoma cells express high levels of *e*N.[50] Our results suggest that *e*N inhibitors are not directly cytotoxic. Nevertheless, they may exhibit anticancer effects in vivo by reducing the production of adenosine and thereby inactivating cytotoxic T cells and inhibiting angiogenesis.[11–15] In future studies, it might be a useful strategy to combine both properties, *e*N inhibition and direct cytotoxicity, by introducing appropriate substituents into the anthraquinone core, to potentially obtain novel anticancer drugs with a dual mechanism of action.

Conclusion

The synthesis and optimization of 4-aryl- and alkyl-amino-substituted anthraquinone derivatives derived from bromaminic acid (**6a**) yielded 17 potent, competitive *e*N inhibitors, 12 of which showed K_i values in the low micromolar range (1–7 μM), while five showed even submicromolar K_i values (0.15–0.6 μM). The most potent compounds proved to be selective versus other investigated *ecto*-nucleotidases and P2 receptors. The new, potent *e*N inhibitors can now be used to study the potential of *e*N as a novel drug target, for example, for the treatment of hepatic fibrosis and cancer. The anthraquinone scaffold appears to be a privileged structure in the medicinal chemistry of nucleotide binding protein targets.

Experimental Section

General. All materials were used as purchased (Sigma-Aldrich or Acros, Germany). Thin-layer chromatography (TLC) was performed using TLC aluminum sheets silica gel 60 F_{254} or TLC aluminum sheets RP silica gel 18 F_{254} (Merck, Darmstadt, Germany). Colored compounds were visible at daylight; other compounds were visualized under UV light (254 nm). Flash chromatography was performed on a Büchi system using silica gel RP-18 (Merck). [1]H and ^{13}C nuclear magnetic resonance (NMR) data were collected on a Bruker Avance 500 MHz NMR spectrometer at 500 (^{1}H) or 126 MHz (^{13}C), respectively. DMSO-d_6 was used as a solvent. Chemical shifts are reported in parts per million (ppm) relative to the deuterated solvent, that is, DMSO, δ [1]H: 2.49 ppm, [13]C: 39.7 ppm; coupling constants J are given in Hertz, and spin multiplicities are given as s (singlet), d (doublet), t (triplet), q (quartet), m (multiplet), or br (broad).

The purities of isolated products were determined by electrospray ionization (ESI)–mass spectra obtained on an liquid chromatography–mass spectrometry (LC-MS) instrument (Applied Biosystems API 2000 LCMS/MS, HPLC Agilent 1100) using the following procedure: The compounds were dissolved at a concentration of 0.5 mg/mL in H_2O:MeOH = 1:1, containing 2 mM NH_4CH_3COO. Then, 10 μL of the sample was injected into an HPLC column (Phenomenix Luna 3 μ C18, 50 mm × 2.00 mm). Elution was performed with a gradient of water:methanol (containing 2 mM NH_4CH_3COO) from 90:10 to 0:100 for 30 min at a flow rate of 250 μL/min, starting the gradient after 10 min. UV absorption was detected from 200 to 950 nm using a diode array detector. The purity of the compounds was determined at 254 nm. For microwave reactions, a CEM Focused Microwave Synthesis type Discover apparatus was used. A freeze dryer (CHRIST ALPHA 1-4 LSC) was used for lyophilization. A second HPLC method was used as previously described.[33] The purity of the compounds proved to be ≥95%. For microwave reactions, a CEM Focused Microwave Synthesis type Discover apparatus was used. A freeze dryer

(CHRIST ALPHA 1-4 LSC) was used for lyophilization. The syntheses of compounds **5, 7–10, 15–20, 22–25, 27–29, 31–43, 46, 49, 50, 53, 62**, and **63** were previously described.[32,33,35,48,49] All other compounds were newly prepared in analogy to the described method.[49]

General Procedure. To a 5 mL microwave reaction vial equipped with a magnetic stirring bar were added bromaminic acid sodium salt (0.081 g, 0.20 mmol) and the appropriate aniline and/or amine derivative (0.40 mmol), followed by a buffer solution of Na_2HPO_4 (pH 9.6) (4 mL) and NaH_2PO_4 (pH 4.2) (1 mL). A catalytic amount (ca. 0.002–0.003 g) of finely powdered elemental copper was added. The mixture was capped and irradiated in the microwave oven for 5–24 min at 100–120 °C. Then, the reaction mixture was cooled to room temperature, and the product was purified using the following procedure. Water (ca. 200 mL) was added to the reaction mixture, and the aqueous solution was extracted with dichloromethane (200 mL). The extraction procedure was repeated until the dichloromethane layer became colorless (2–3 times). Then, the aqueous layer was reduced by rotary evaporation to a volume of 10–20 mL, which was subsequently submitted to flash column chromatography using RP-18 silica gel and water as an eluent. The purity of the products proved to be ≥95% as determined by LC-MS and HPLC using two different systems. The pooled product-containing fractions were evaporated under vacuum to remove the methanol, and the remaining water was subsequently removed by lyophilization to yield up to 90% isolated yield of product as blue powders.

Spectral Data of Key Compounds. Sodium 1-Amino-4-(4-hydroxyphenylamino)-9,10-dioxo-9,10-dihydroanthracene-2-sulfonate (23). According to the general procedure: 10 min, 120 °C, 80 W; pressure up to 10 bar. Analytical data: mp > 300 °C, blue powder. ^{1}H NMR: δ 6.82 (d, 2H, 2′-H, 6′-H), 7.08 (d, 2H, 3′-H, 5′-H), 7.81 (s, 1H, 3-H), 7.83 (m, 2H, 6-H, 7-H), 8.27 (m, 2H, 5-H, 8-H), 10.15 (br, 2H, 1-NH$_2$), 12.05 (s, 1H, 4-NH). ^{13}C NMR: δ 108.97 (C-9a), 110.03 (C-4a), 116.39 (C-2′, C6′), 122.93 (C-3), 125.98 (C-5), 126.13 (C-8), 126.36 (C-3′, C5′), 129.98 (C-1′), 132.75 (C-6), 132.96 (C-7), 133.90 (C-10a), 134.29 (C-8a), 143.22 (C-4), 143.25 (C-2), 144.19 (C-1), 155.52 (C-4′), 181.69 (C-9), 181.70 (C-10). LC-MS (m/z): 411 [M − Na]$^+$, 409 [M − Na]$^-$. Purity by HPLC-UV (254 nm)-ESI-MS: 97.3%.

Sodium 1-Amino-4-(4-aminophenylamino)-9,10-dioxo-9,10-dihydroanthracene-2-sulfonate (33). According to the general procedure: 5 min, 100 °C, 60 W; pressure up to 10 bar. Analytical data: mp > 300 °C, blue powder. ^{1}H NMR: δ 5.17 (bs, 2H, 4′-NH$_2$), 6.64 (d, 2H, 2′-H, 6′-H), 6.94 (d, 2H, 3′-H, 5′-H), 7.81 (s, 1H, 3-H), 7.82 (m, 2H, 6-H, 7-H), 8.27 (m, 2H, 5-H, 8-H), 10.17 (br, 2H, 1-NH$_2$), 12.09 (s, 1H, 4-NH). ^{13}C NMR: δ 108.84 (C-9a), 109.52 (C-4a), 114.78 (C-2′, C6′), 122.85 (C-3), 125.93 (C-5), 126.09 (C-8), 126.14 (C-1′), 126.82 (C-3′, C5′), 132.65 (C-6), 132.75 (C-7), 133.99 (C-10a), 134.26 (C-8a), 143.24 (C-4), 143.88 (C-2), 144.15 (C-1), 147.08 (C-4′), 181.17 (C-9), 181.52 (C-10). LC-MS (m/z): 432 [M]$^+$, 427 [M − Na + NH$_4$$^+$]$^+$, 410 [M − Na]$^+$, 408 [M − Na]$^-$. Purity by HPLC-UV (254 nm)-ESI-MS: 95.7%.

Sodium 1-Amino-4-(2-carboxy-4-fluorophenylamino)-9,10-dioxo-9,10-dihydroanthracene-2-sulfonate (45). According to the general procedure: 5 min, 120 °C, 100 W; pressure up to 10 bar. Analytical data: mp > 300 °C, blue powder. ^{1}H NMR: δ 7.25 (b, 2H, 3′-H, 5′-H), 7.63 (m, 1H, 6′-H), 7.83 (m, 2H, 6-H, 7-H), 8.06 (s, 1H, 3-H), 8.26 (m, 2H, 5-H, 8-H), 9.99 (br, 2H, 1-NH$_2$), 12.49 (s, 1H, 4-NH). ^{13}C NMR: δ 110.1, 113.6 (C-9a, C-4a), 114.9, 116.8, (C-2′, C-6′), 117.2, 117.8, 122.5, 124.7, 126.1, 126.2 (C-3, C-5, C-8, C-4′, C-5′, C-3′), 133.0, 133.2, 133.9, 134.2, (C-8a, C-10a, C-6, C-7) 137.6 (C-1′), 137.7 (C-4), 141.5, 144.8 (C-1, C-2), 182.0 (C-9), 182.5 (C-10). LC-MS (m/z): 474 [M − Na + NH$_4$$^+$]$^+$, 457 [M − Na]$^+$, 455 [M − Na]$^-$. Purity by HPLC-UV (254 nm)-ESI-MS: 97.0%.

Sodium 1-Amino-4-(2-anthracenylamino)-9,10-dioxo-9,10-dihydroanthracene-2-sulfonate (52). According to the general

procedure: 5 min, 120 °C, 100 W; pressure up to 10 bar. Analytical data: mp > 300 °C, blue powder. ^{1}H NMR: δ 7.49 (m, 3H, 3 anthracene H), 7.87 (m, 3H, 6-H, 7-H, 1 anthracene H), 8.06 (dd, 2H, 2 anthracene H), 8.16 (d, 1H, 1 anthracene H), 8.22 (s, 1H, 3-H), 8.29 (m, 2H, 5-H, 8-H), 8.45 (br, 1H, 1 anthracene H), 8.57 (br, 1H, 1 anthracene H), 10.10 (br, 2H, 1-NH$_2$), 12.17 (s, 1H, NH). ^{13}C NMR: δ 109.5, 112.5 (C-4a, C-9a), 117.1, 123.4 (C-2′, C-4′), 123.7 (C-3), 124.9, 125.3, 126.0, 126.1, 126.2, 126.3, 127.9, 128.3, 129.9, 130.0, 130.8, 131.9, (C-5, C-8, C-5′, C-6′, C-7′, C-8′, C-4a′, C-8a′, C-9′, C-10′, C-9a′, C-10a′), 132.0, 133.0, 133.4, 133.7, 134.3, 136.8, (C-6, C-7, C-8a, C-10a, C-1′, C-3′), 140.0, 142.8, 144.8 (C-1, C-2, C-4), 182.1 (C-9), 182.9 (C-10). LC-MS (m/z): 495 [M − Na]$^+$, 493 [M − Na]$^-$. Purity by HPLC-UV (254 nm)-ESI-MS: 96.5%.

Sodium 1-Amino-4-(1-naphthylamino)-9,10-dioxo-9,10-dihydroanthracene-2-sulfonate (53). According to the general procedure: 5 min, 120 °C, 100 W; pressure up to 10 bar. Analytical data: mp > 300 °C, blue powder. ^{1}H NMR: δ 7.49 (br, 1H, NH$_2$), 7.50 (d, 1H, ^3J = 7.3 Hz, 1 naphthalene H), 7.60 (m, 3H, 3 naphthalene H); 7.80 (s, 1H, 3-H), 7.87 (m, 3H, 6-H, 7-H, 1 naphthalene H), 8.02, 8.08 (m, 2H, 2 naphthalene H), 8.32 (m, 2H, 5-H, 8-H), 10.12 (br, 2H, 1-NH$_2$), 12.51 (s, 1H, NH). ^{13}C NMR: δ 109.2, 111.4 (C-4a, C-9a), 121.5, 121.9 (C-2′, C-4′), 122.9 (C-3), 125.7, 126.18, 126.21, 126.9, 127.1, 128.6, 129.0 (C-5, C-8, C-5′, C-6′, C-7′, C-8′, C-4a′, C-8a′), 132.9, 133.4, 133.8, 134.4, 134.5, 135.2 (C-6, C-7, C-8a, C-10a, C-1′, C-3′), 142.6, 143.2, 144.5 (C-1, C-2, C-4), 181.9 (C-9), 182.9 (C-10). LC-MS (m/z): 462 [M − Na + NH$_4$$^+$]$^+$, 445 [M − Na]$^+$, 443 [M − Na]$^-$. Purity by HPLC-UV (254 nm)-ESI-MS: 100%.

Biological Assays. CE Instrumentation. All experiments were carried out using a P/ACE MDQ CE system (Beckman Instruments, Fullerton, CA) equipped with a UV detection system coupled with a diode array detector (DAD). Data collection and peak area analysis were performed by the P/ACE MDQ software 32 KARAT obtained from Beckman Coulter. The capillary and sample storing unit temperature were kept constant at 25 °C. The electrophoretic separations were carried out using an eCAP polyacrylamide-coated fused-silica capillary [(30 cm (20 cm effective length) × 50 μm internal diameter (i.d.) × 360 μm outside diameter (o.d.), obtained from CS-Chromatographie (Langerwehe, Germany)]. The separation was performed using an applied current of −60 μA and a data acquisition rate of 8 Hz. Analytes were detected using direct UV absorbance at 260 nm. The capillary was conditioned by rinsing with water for 2 min and subsequently with buffer (phosphate 50 mM, pH 6.5) for 1 min. Sample injections were made at the cathodic side of the capillary.

eN (CD73) Assays. Screening of compounds at the rat eN (K_m = 20 μM) was performed essentially as previously described using a CE method.[50] The enzyme was expressed in Sf9 insect cells as a GST fusion protein and purified by affinity chromatography using agarose-coupled GSH as described.[51] The compounds were initially screened at a concentration of 1 mM. They were dissolved in the reaction buffer (2 mM MgCl$_2$, 1 mM CaCl$_2$, and 10 mM Hepes, pH 7.4) together with the substrate AMP (500 μM). The reaction was initiated by adding 10 μL of recombinant rat eN solution (0.13 μg protein) and was then allowed to proceed at 37 °C for 15 min. After the reaction was stopped by heating at 99 °C for 10 min, aliquots of 50 μL of the reaction mixture were transferred to mini CE vials and injected into the CE instrument. The absorbance at 260 nm was monitored continuously, and the adenosine concentrations were determined from the area under its absorbance peak. For the determination of the K_i values, 6−8 different concentrations of the respective inhibitor spanning about 3 orders of magnitude were used. All experiments were performed three times each in duplicate. The Cheng−Prusoff equation was used to calculate the K_i values from the IC$_{50}$ values, determined by the nonlinear curve fitting program PRISM 4.0 (GraphPad, San Diego, CA).

Determination of NTPDase Inhibition. NTPDase inhibition was monitored by a CE method as previously described.[35,62]

Enzyme assays were carried out at 37 °C in a final volume of 100 μL. The reaction mixture contained 140 mM NaCl, 5 mM KCl, 1 mM MgCl$_2$, 2 mM CaCl$_2$, 10 mM Hepes, pH 7.4, and 400 μM ATP. Different concentrations of inhibitors dissolved in water or containing 1% DMSO in cases of low water solubility when a stock solution could not be prepared in water (10 μL) were added, and the reaction was initiated by the addition of 10 μL of the appropriately diluted membrane preparations containing NTPDase1, NTPDase2, or NTPDase3, respectively. The mixture was incubated for 10 min, and the reaction was terminated by heating at 99 °C for 5 min. Aliquots of the reaction mixture (50 μL) were then diluted 10-fold with water containing UMP (final concentration, 20 μM) as an internal standard, transferred to mini-CE vials, injected into the CE instrument, and separated as described.[62] Each analysis was repeated three times (triplicates) in two separate experiments.

Experimental Procedures for Testing of Compounds at P2Y$_2$, P2Y$_4$, and P2Y$_6$ Receptors. Astrocytoma cell lines stably transfected with either the human P2Y$_2$, the human P2Y$_4$, or the rat P2Y$_6$ receptor were used.[32,62−64] Test compounds were investigated by measuring their inhibition of P2Y$_2$, P2Y$_4$, or P2Y$_6$ receptor-mediated intracellular calcium mobilization using a FLUOstar plate reader or a NOVOstar plate reader, respectively (BMG LabTechnologies, Offenburg, Germany) as previously described.[32,62,64−66] Cells were loaded with Fura-2 AM (Molecular Probes, Eugene, OR). Cell aliquots (160 μL per well) were then preincubated with test compound (20 μL per well) for at least 20 min before injection of the physiological ligand (1 μM UTP for the P2Y$_2$, 3 μM UTP for the P2Y$_4$, and 3 μM UDP for the P2Y$_6$ receptor, 20 μL per well). The final volume was 200 μL per well. Fluorescence was measured at 520 nm (bandwidth 20 nm) after excitation at 320 nm for 56 intervals of 0.4 s each. For compounds that showed an inhibition of more than 40% at a concentration of 10 μM, full curves were determined with seven or eight different concentrations spanning 3 orders of magnitude to determine IC$_{50}$ values. Three separate experiments were performed, each in triplicate, unless otherwise noted. IC$_{50}$ values for antagonists were calculated by nonlinear regression using Prism 4.0 (GraphPad Software, San Diego, CA).

Molecular Modeling Studies. A possible binding mode of the strongest inhibitor, compound **52**, to rat eN was investigated by molecular modeling using a comparative molecular model, as described in the Results and Discussion. The model was evaluated using Ramachandran and sequence-structure compatibility analysis carried out with ProSA II.[67,68] The Ramachandran diagram of rat eN revealed that over 90% of residues are located in the most favored regions. The ProSA Z-score (−8.47) is comparable to the template Z-score (−10.91). Initially, we superimposed compound **52** onto the structurally corresponding parts of **2** (AOPCP). In the next step, van der Waals (vdW) contacts between compound **52** and active site residues were analyzed using MOE. The anthraquinone substructure of compound **52** formed short contacts with Leu 186, Glu 450, and Thr 448. To generate a plausible fit of compound **52** within the active site, we subjected all residues within 4.5 Å of compound **52** to controlled energy minimization with MOE [and the Assisted Model Building with Energy Refinement (AMBER) 99 force field], except the two zinc coordination spheres that were held fixed. During conjugate gradients minimization, backbone and side chain atoms within 4.5 Å of the inhibitor were tethered. During final minimization steps, only inhibitor atoms were allowed to move to achieve high steric complementarity to the active site. Only minor changes in atomic positions of a few eN residues were required to adapt the active site to compound **52** and to remove all unfavorable steric contacts.

Supporting Information Available: Analytical data and ^{1}H NMR, ^{13}C NMR, and LC-MS spectra of the newly synthesized anthraquinone derivatives. This material is available free of charge via the Internet at http://pubs.acs.org.

References

(1) (a) Burnstock, G. Physiology and pathophysiology of purinergic neurotransmission. *Physiol. Rev.* **2007**, *87*, 659–797. (b) Burnstock, G. Pathophysiology and therapeutic potential of purinergic signaling. *Pharmacol. Rev.* **2006**, *58*, 58–86. (c) Müller, C. E. P2-pyrimidinergic receptors and their ligands. *Curr. Pharm. Des.* **2002**, *8*, 2353–2369. (d) Brunschweiger, A.; Müller, C. E. P2 receptors activated by uracil nucleotides—An update. *Curr. Med. Chem.* **2006**, *13*, 289–312.

(2) (a) Bender, E.; Buist, A.; Jurzak, M.; Langlois, X.; Baggerman, G.; Verhasselt, P.; Ercken, M.; Guo, H. Q.; Wintmolders, C.; Van, d. W.I.; Van, O. I.; Schoofs, L.; Luyten, W. Characterization of an orphan G protein-coupled receptor localized in the dorsal root ganglia reveals adenine as a signaling molecule. *Proc. Natl. Acad. Sci. U.S.A.* **2002**, *99*, 8573–8578. (b) Gorzalka, S.; Vittori, S.; Volpini, R.; Cristalli, G.; von Kügelgen, I.; Müller, C. E. Evidence for the Functional Expression and Pharmacological Characterization of Adenine Receptors in Native Cells and Tissues. *Mol. Pharmacol.* **2005**, *67*, 955–964. (c) von Kügelgen, I.; Schiedel, A. C.; Hoffmann, K.; Alsdorf, B. A.; Abdelrahman, A.; Müller, C. E. Cloning and Functional Expression of a Novel G_i Protein-Coupled Receptor for Adenine from Mouse Brain. *Mol. Pharmacol.* **2008**, *73*, 469–477. (d) Borrmann, T.; Abdelrahman, A.; Volpini, R.; Lambertucci, C.; Alksnis, E.; Gorzalka, S.; Knospe, M.; Schiedel, A. C.; Cristalli, G.; Müller, C. E. Structure—Activity Relationships of Adenine and Deazaadenine Derivatives as Ligands for Adenine Receptors, a New Purinergic Receptor Family. *J. Med. Chem.* **2009**, *52*, 5974–5989.

(3) Burnstock, G. Purinergic cotransmission. *Brain Res. Bull.* **1999**, *50*, 355–357.

(4) Zimmermann, H.; Braun, N. Ecto-nucleotidases: Molecular structures, catalytic properties, and functional roles in the nervous system. *Prog. Brain Res.* **1999**, *120*, 371–385.

(5) Kukulski, F.; Lévesque, S. A.; Lavoie, E. G.; Lecka, J.; Bigonnesse, F.; Knowles, A. F.; Robson, S. C.; Kirley, T. L.; Sévigny, J. Comparative hydrolysis of P2 receptor agonists by NTPDases 1, 2, 3, and 8. *Purinergic Signalling* **2005**, *1*, 193–204.

(6) Zimmermann, H. 5′-nucleotidase: Molecular structure and functional aspects. *Biochem. J.* **1992**, *285*, 345–365.

(7) Zimmermann, H. Extracellular metabolism of ATP and other nucleotides. *Naunyn-Schmiedeberg's Arch. Pharmacol.* **2000**, *362*, 299–309.

(8) Napieralski, R.; Kempkes, B.; Gutensohn, W. Evidence for co-ordinated induction and repression of ecto-5′-nucleotidase (CD73) and the A_{2A} adenosine receptor in a human B cell line. *Biol. Chem. Hoppe—Seyler* **2003**, *384*, 483–487.

(9) Goding, J. W.; Grobben, B.; Slegers, H. Physiological and pathophysiological functions of the ecto-nucleotide pyrophosphatase/phosphodiesterase family. *Biochim. Biophys. Acta* **2003**, *1638*, 1–19.

(10) Sadej, R.; Spychala, J.; Skladanowski, A. C. Expression of ecto-5′-nucleotidase (eN, CD73) in cell lines from various stages of human melanoma. *Melanoma Res.* **2006**, *16*, 213–222.

(11) Resta, R.; Yamashita, Y.; Thompson, L. F. Ecto-enzyme and signaling functions of lymphocyte CD73. *Immunol. Rev.* **1998**, *161*, 95–109.

(12) Spychala, J. Tumor-promoting functions of adenosine. *Pharmacol. Ther.* **2000**, *87*, 161–173.

(13) (a) Mikhailov, A.; Sokolovskaya, A.; Yegutkin, G. G.; Amdahl, H.; West, A.; Yagita, H.; Lahesmaa, R.; Thompson, L. F.; Jalkanen, S.; Blokhin, D.; Eriksson, J. E. CD73 participates in cellular multiresistance program and protects against TRAIL-induced apoptosis. *J. Immunol.* **2008**, *181*, 464–475. (b) Ujházy, P.; Berleth, E. S.; Pietkiewicz, J. M.; Kitano, H.; Skaar, J. R.; Ehrke, M. J.; Mihich, E. Evidence for the involvement of ecto-5′-nucleotidase (CD73) in drug resistance. *Int. J. Cancer* **1996**, *68*, 493–500.

(14) Braganhol, E.; Tamajusuku, A. S.; Bernardi, A.; Wink, M. R.; Battastini, A. M. Ecto-5′-nucleotidase/CD73 inhibition by

(15) Zhi, X.; Chen, S.; Zhou, P.; Shao, Z.; Wang, L.; Ou, Z.; Yin, L. RNA interference of ecto-5′-nucleotidase (CD73) inhibits human breast cancer cell growth and invasion. *Clin. Exp. Metastasis* **2007**, *24*, 439–448.

(16) (a) Crane, J. K.; Naeher, T. M.; Shulgina, I.; Zhu, C.; Boedeker, E. C. Effect of zinc in enteropathogenic *Escherichia coli* infection. *Infect. Immun.* **2007**, *75*, 5974–5984. (b) Alam, M. S.; Kurtz, C. C.; Rowlett, R. M.; Reuter, B. K.; Wiznerowicz, E.; Das, S.; Linden, J.; Crowe, S. E.; Ernst, P. B. CD73 is expressed by human regulatory T helper cells and suppresses proinflammatory cytokine production and Helicobacter felis-induced gastritis in mice. *J. Infect. Dis.* **2009**, *199*, 494–504.

(17) Peng, Z.; Fernandez, P.; Wilder, T.; Yee, H.; Chiriboga, L.; Chan, E. S.; Cronstein, B. N. Ecto-5′-nucleotidase (CD73)-mediated extracellular adenosine production plays a critical role in hepatic fibrosis. *FASEB J.* **2008**, *22*, 2263–2272.

(18) (a) Kawashima, Y.; Nagasawa, T.; Ninomiya, H. Contribution of ecto-5′-nucleotidase to the inhibition of platelet aggregation by human endothelial cells. *Blood* **2000**, *96*, 2157–2162. (b) Sträter, N. Ecto-5′-nucleotidase: Structure function relationships. *Purinergic Signalling* **2006**, *2*, 343–350.

(19) Uchino, K.; Matsuo, T.; Iwamoto, M.; Tonosaki, Y.; Fukuchi, A. New 5′-nucleotidase inhibitors, NPF-86IA, NPF-86IB, NPF-86IIA, and NPF-86IIB from Areca catechu; Part I. Isolation and biological properties. *Planta Med.* **1988**, *54*, 419–422.

(20) Braganhol, E.; Tamajusuku, A. S.; Bernardi, A.; Wink, M. R.; Battastini, A. M. Ecto-5′-nucleotidase/CD73 inhibition by quercetin in the human U138MG glioma cell line. *Biochim. Biophys. Acta* **2007**, *1770*, 1352–1359.

(21) Bo, X.; Fischer, B.; Maillard, M.; Jacobson, K. A.; Burnstock, G. Comparative studies on the affinities of ATP derivatives for P2X-purinoceptors in rat urinary bladder. *Br. J. Pharmacol.* **1994**, *112*, 1151–1159.

(22) (a) Bültmann, R.; Starke, K. P2-purinoceptor antagonists discriminate three contraction mediating receptors for ATP in rat vas deferens. *Naunyn-Schmiedeberg's Arch. Pharmacol.* **1994**, *349*, 74–80. (b) Tuluc, F.; Bültmann, R.; Glänzel, M.; Frahm, A. W.; Starke, K. P2-receptor antagonists: IV. Blockade of P2-receptor subtypes and ecto-nucleotidases by compounds related to reactive blue 2. *Naunyn-Schmiedeberg's Arch. Pharmacol.* **1998**, *357*, 111–120.

(23) Brake, A. J.; Wagenbach, M. J.; Julius, D. New structural motif for ligand-gated ion channels defined by an ionotropic ATP receptor. *Nature* **1994**, *371*, 519–523.

(24) (a) Simon, J.; Webb, T. E.; King, B. F.; Burnstock, G.; Barnard, E. A. Characterisation of a recombinant P2Y purinoceptor. *Eur. J. Pharmacol.* **1995**, *291*, 281–289. (b) Chang, K.; Hanoka, K.; Kumada, M.; Takuwa, Y. Molecular cloning and functional analysis of a novel P2 nucleotide receptor. *J. Biol. Chem.* **1995**, *270*, 26152–26158.

(25) Communi, D.; Parmentier, M.; Boeynaems, J.-M. Cloning, functional expression and tissue distribution of the human $P2Y_6$ receptor. *Biochem. Biophys. Res. Commun.* **1996**, *222*, 303–308.

(26) Communi, D.; Robaye, B.; Boeynaems, J.-M. Pharmacological characterization of the human $P2Y_{11}$ receptor. *Br. J. Pharmacol.* **1999**, *128*, 1199–1206.

(27) Michel, A. D.; Grahames, C. B. A.; Humphrey, P. P. A. Functional characterization of P2 purinoceptors in PC12 cells by measurement of radiolabelled calcium influx. *Naunyn-Schmiedeberg's Arch. Pharmacol.* **1996**, *354*, 562–571.

(28) Seguela, P.; Haghigi, A.; Soghommonian, J.-J.; Cooper, E. A novel neuronal P2X ATP receptor ion channel with widespread distribution in the brain. *J. Neurosci.* **1996**, *15*, 448–455.

(29) Webb, T. E.; Feolde, E.; Vigne, P.; Neary, J. T.; Runberg, A.; Frelin, C.; Barnard, E. A. The P2Y purinoceptor in rat brain microvascular endothelial cells couple to inhibition of adenylate cyclase. *Br. J. Pharmacol.* **1996**, *119*, 1385–1392.

(30) Glänzel, M.; Bültmann, R.; Starke, K.; Frahm, A. W. Structure-activity relationships of novel P2-receptor antagonists structurally related to Reactive Blue 2. *Eur. J. Med. Chem.* **2005**, *40*, 1262–1276.

(31) Glänzel, M.; Bültmann, R.; Starke, K.; Frahm, A. W. Constitutional isomers of Reactive Blue 2—Selective P2Y-receptor antagonists? *Eur. J. Med. Chem.* **2003**, *38*, 303–312.

(32) Weyler, S.; Baqi, Y.; Hillmann, P.; Kaulich, M.; Hunder, A. M.; Müller, I. A.; Müller, C. E. Combinatorial synthesis of anilinoanthraquinone derivatives and evaluation as non nucleotide-derived $P2Y_2$ receptor antagonists. *Bioorg. Med. Chem. Lett.* **2008**, *18*, 223–227.

(33) Baqi, Y.; Atzler, K.; Köse, M.; Glänzel, M.; Müller, C. E. High-Affinity, Non-Nucleotide-Derived Competitive Antagonists of Platelet $P2Y_{12}$ Receptors. *J. Med. Chem.* **2009**, *52*, 3784–3793.

(34) Hoffmann, K.; Baqi, Y.; Morena, M. S.; Glänzel, M.; Müller, C. E.; von Kügelgen, I. Interaction of new, very potent non-nucleotide antagonists with Arg256 of the human platelet P2Y$_{12}$-receptor. *J. Pharmacol. Exp. Ther.* **2009**, *331*, 648–655.

(35) Baqi, Y.; Weyler, S.; Iqbal, J.; Zimmermann, H.; Müller, C. E. Structure-activity relationships of anthraquinone derivatives derived from bromaminic acid as inhibitors of ectonucleoside triphosphate diphosphohydrolases (E-NTPDases). *Purinergic Signalling* **2009**, *5*, 91–106.

(36) Glänzel, M.; Bültmann, R.; Starke, K.; Frahm, A. W. Members of the acid blue 129 family as potent and selective P2Y-receptor antagonists. *Drug Dev. Res.* **2003**, *59*, 64–71.

(37) Evans, B. E.; Rittle, K. E.; Bock, M. G.; DiPardo, R. M.; Freidinger, R. M.; Whitter, W. L.; Lundell, G. F.; Veber, D. F.; Anderson, P. S.; Chang, R. S. L.; Lotti, V. J.; Cerino, D. J.; Chen, T. B.; Kling, P. J.; Kunkel, K. A.; Springer, J. P.; Hirshfieldt, J. Methods for Drug Discovery: Development of Potent, Selective, Orally Effective Cholecystokinin Antagonists. *J. Med. Chem.* **1988**, *31*, 2235–2246.

(38) Daly, J. W. Caffeine analogs: Biomedical impact. *Cell. Mol. Life Sci.* **2007**, *64*, 2153–2169.

(39) Kroeck, F. W.; Neeff, R.; Scheiter, H. 1,4-Diamino-2,3-dicyanoanthraquinones; EP 23645, CAN 95:8807; Bayer A.-G.: Germany, 1981; 17 pp.

(40) Weinand, K. 1-Amino-4-pentamethyleneamineanthraquinone-2-sulfonic acid. U.S. 1688256, CAN 23:2045; Grasselli Dyestuff Corp., 1928.

(41) Oprisan, L.; Slavila, N.; Sebe, I. Bromamine acid derivated anthraquinone dyes. *Sci. Bull. - Univ. "Politeh." Bucharest, Ser. B* **2007**, *69*, 43–48.

(42) Horyna, J.; Slosar, P.; Popova, E.; Znamenacek, M. Preparation of 1-amino-4-(aryl- or alkylamino)-2-anthraquinonesulfonic acids and their salts. CS 256876, Czech., 1989; 8 pp.

(43) Adam, J. M.; Bloch, P. Anthraquinone dyes. EP 103541 A2; Ciba-Geigy A.-G.: Switzerland, 1984; 20 pp.

(44) Skowronski, R.; Omakowska, J. Anthrapyridone derivative dyes. PL 107974; Uniwersytet Lodzki: Poland, 1980; 2 pp.

(45) 6-Amino-10-bromonaphth[2,3-c]acridan-5,8,14-trione. GB 775802; Farbenfabriken Bayer A.-G.: Germany, 1957.

(46) Fisichella, S.; Occhipinti, S. Thermodynamics of dyeing of anthraquinonoid dyes for Viscose Rayon. *Ann. Chim.* **1978**, *68*, 503–506.

(47) Murata, K.; Harada, K. Acid anthraquinone dyes. I. *Hiroshima Daigaku Kogakubu Kenkyu Hokoku* **1954**, *3*, 135–139.

(48) Baqi, Y.; Müller, C. E. Catalyst-Free Microwave-Assisted Amination of 2-Chloro-5-nitrobenzoic Acid. *J. Org. Chem.* **2007**, *72*, 5908–5911.

(49) Baqi, Y.; Müller, C. E. Rapid and Efficient Microwave-Assisted Copper(0)-Catalyzed Ullmann Coupling Reaction: General Access to Anilinoanthraquinone Derivatives. *Org. Lett.* **2007**, *9*, 1271–1274.

(50) Iqbal, J.; Jirovsky, D.; Lee, S. Y.; Zimmermann, H.; Müller, C. E. Capillary electrophoresis-based nanoscale assays for monitoring ecto-5′-nucleotidase activity and inhibition in preparations of recombinant enzyme and melanoma cell membranes. *Anal. Biochem.* **2008**, *373*, 129–140.

(51) Servos, J.; Reiländer, H.; Zimmermann, H. Catalytically active soluble ecto-5′-nucleotidase purified after heterologous expression as a tool for drug screening. *Drug Dev. Res.* **1999**, *45*, 269–276.

(52) Berman, H. M.; Westbrook, J.; Feng, Z.; Gilliland, G.; Bhat, T. N.; Weissig, H.; Shindyalov, I. N.; Bourne, P. E. The protein data bank. *Nucleic Acids Res.* **2000**, *28*, 235–242.

(53) Molecular Operating Environment (MOE 2007.09); C.C.G.: Montreal, Quebec, Canada, 2007.

(54) Rarey, B.; Kramer, T.; Lengauer, G.; Klebe, G. A fast flexible docking method using an incremental construction algorithm. *J. Mol. Biol.* **1996**, *261*, 470–489.

(55) FlexX 2.2.1, BioSolve IT GmbH, An der Ziegelei 75, 53757 St. Augustin, Germany.

(56) Minotti, G.; Menna, P.; Salvatorelli, E.; Cairo, G.; Gianni, L. Anthracyclines: molecular advances and pharmacologic developments in antitumor activity and cardiotoxicity. *Pharmacol. Rev.* **2004**, *56*, 185–229.

(57) Shchekotikhin, A. E.; Glazunova, V. A.; Dezhenkova, L. G.; Luzikov, Y. N.; Sinkevich, Y. B.; Kovalenko, L. V.; Buyanov, V. N.; Balzarini, J.; Huang, F.-C.; Lin, J.-J.; Huang, H.-S.; Shtil, A. A.; Preobrazhenskaya, M. N. Synthesis and cytotoxic properties of 4,11-bis[(aminoethyl)amino]anthrax[2,3-b]thiophene-5,10-diones, novel analogues of antitumor anthracene-9,10-diones. *Bioorg. Med. Chem.* **2009**, *17*, 1861–1869.

(58) Butterworth, B. E.; Mathre, O. B.; Ballinger, K. E.; Adalsteinsson, O. Contamination is a frequent confounding factor in toxicology studies with anthraquinone and related compounds. *Int. J. Toxicol.* **2004**, *23*, 335–344.

(59) Venitt, S.; Crofton-Sleigh, C.; Agbandje, M.; Jenkins, T. C.; Neidle, S. Anthracene-9,10-diones as Potential Anticancer Agents: Bacterial Mutation Studies of Amido-Substituted Derivatives Reveal an Unexpected Lack of Mutagenicity. *J. Med. Chem.* **1998**, *41*, 3748–3752.

(60) Su, H.-Y.; Cherng, S.-H.; Chen, C.-C.; Lee, H. Emodin inhibits the mutagenicity and DNA adducts induced by 1-nitropyrene. *Mutat. Res.* **1995**, *329*, 205–212.

(61) World Health Organization, International Agency for Research on Cancer. Polynuclear aromatic compounds, part 1, chemical, environmental and experimental data. *IARC Monographs on the Evaluation of Carcinogenic Risks to Humans*; World Health Organization: Geneva, Switzerland, 1983; Vol. 32 (http://monographs.iarc.fr/ENG/Monographs/vol32/volume32.pdf).

(62) Brunschweiger, A.; Iqbal, J.; Umbach, F.; Scheiff, A. B.; Munkonda, M. N.; Sévigny, J.; Knowles, A. F.; Müller, C. E. Selective nucleoside triphosphate diphosphohydrolase-2 (NTPDase 2) inhibitors: Nucleotide mimetics derived from uridine-5′-carboxamide. *J. Med. Chem.* **2008**, *51*, 4518–4528.

(63) Charlton, S. J.; Brown, C. A.; Weisman, G. A.; Turner, J. T.; Erb, L.; Boarder, M. R. Cloned and transfected P2Y$_4$ receptors: characterization of a suramin and PPADS-insensitive response to UTP. *Br. J. Pharmacol.* **1996**, *119*, 1301–1303.

(64) Hillmann, P.; Ko, G.-Y.; Spinrath, A.; Raulf, A.; von Kügelgen, I.; Wolff, S. C.; Nicholas, R. A.; Kostenis, E.; Höltje, H.-D.; Müller, C. E. Key Determinants of Nucleotide-Activated G Protein-Coupled P2Y$_2$ Receptor Function Revealed by Chemical and Pharmacological Experiments, Mutagenesis and Homology Modeling. *J. Med. Chem.* **2009**, *52*, 2762–2775.

(65) Kaulich, M.; Streicher, F.; Mayer, R.; Müller, I.; Müller, C. E. Flavonoids−Novel lead compounds for the development of P2Y$_2$ receptor antagonists. *Drug Dev. Res.* **2003**, *59*, 72–81.

(66) Kassack, M. U.; Höfgen, B.; Lehmann, J.; Eckstein, N.; Quillan, J. M.; Sadee, W. Functional screening of G protein-coupled receptors by measuring intracellular calcium with a fluorescence microplate reader. *J. Biomol. Screen.* **2002**, *7*, 233–246.

(67) Wiederstein, M.; Sippl, M. J. ProSA-web: Interactive web service for the recognition of errors in three-dimensional structures of proteins. *Nucleic Acids Res.* **2007**, *35*, W407–W410.

(68) Sippl, M. J. Recognition of errors in three-dimensional structures of proteins. *Proteins* **1993**, *17*, 355–362.